

This is the accepted manuscript made available via CHORUS. The article has been published as:

## Temperature-induced decay of persistent currents in a superfluid ultracold gas

A. Kumar, S. Eckel, F. Jendrzejewski, and G. K. Campbell

Phys. Rev. A **95**, 021602 — Published 24 February 2017

DOI: [10.1103/PhysRevA.95.021602](https://doi.org/10.1103/PhysRevA.95.021602)

# Temperature induced decay of persistent currents in a superfluid ultracold gas

A. Kumar, S. Eckel, F. Jendrzejewski, and G. K. Campbell\*  
*Joint Quantum Institute, National Institute of Standards and Technology  
 and University of Maryland, Gaithersburg, Maryland 20899, USA*  
 (Dated: January 23, 2017)

We study how temperature affects the lifetime of a quantized, persistent current state in a toroidal Bose-Einstein condensate (BEC). When the temperature is increased, we find a decrease in the persistent current lifetime. Comparing our measured decay rates to simple models of thermal activation and quantum tunneling, we do not find agreement. We also measured the size of hysteresis loops size in our superfluid ring as a function of temperature, enabling us to extract the critical velocity. The measured critical velocity is found to depend strongly on temperature, approaching the zero temperature mean-field solution as the temperature is decreased. This indicates that an appropriate definition of critical velocity must incorporate the role of thermal fluctuations, something not explicitly contained in traditional theories.

Persistent currents invoke immense interest due to their long lifetimes, and they exist in a number of diverse systems, such as superconductors [1, 2], liquid helium [3, 4], dilute ultracold gases [5–7] and polariton condensates [8]. Superconductors in a multiply connected geometry exhibit quantization of magnetic flux, [9] while the persistent current states in a superfluid are quantized in units of  $\hbar$ , the reduced Planck constant. To create transitions between quantized persistent current states, the critical velocity of a superfluid (or critical current of a superconductor) must be exceeded. In ultracold gases, the critical velocity is typically computed at zero-temperature, whereas experiments are obviously performed at non-zero temperature. In this work, we experimentally investigate the role of temperature in the decay of persistent currents in ultracold-atomic, superfluid rings (Fig. 1a).

In the context of the free energy of the system, different persistent current states of the system (denoted by an integer  $\ell$  called the winding number) can be described by local energy minima, separated by energy barriers (here, we concentrate on  $\ell = 0$  and  $\ell = 1$  shown in Fig.1(b)) [10, 11]. The metastable behavior emerges from the energy barrier,  $E_b$ , between two persistent current states. For superconducting rings, the decay dynamics have been understood by the Caldeira-Leggett model [12]: the decay occurs either via quantum tunneling through the energy barrier or thermal activation over the top of the barrier. When first investigated in superconductors [13–19], the decay rate from the metastable state  $\Gamma$  was fit to an escape temperature  $T_{\text{esc}}$  by the relation  $\Gamma = \Omega_a \exp(-E_b/k_B T_{\text{esc}})$ , where  $k_B$  is the Boltzmann constant. In the context of the WKB approximation in quantum mechanics or the Arrhenius equation in thermodynamics,  $\Omega_a$  represents the “attempt frequency”: i.e. how often the system attempts to overcome the barrier. The  $\exp(-E_b/k_B T_{\text{esc}})$  represents the probability of surmounting the barrier on any given attempt. The prob-

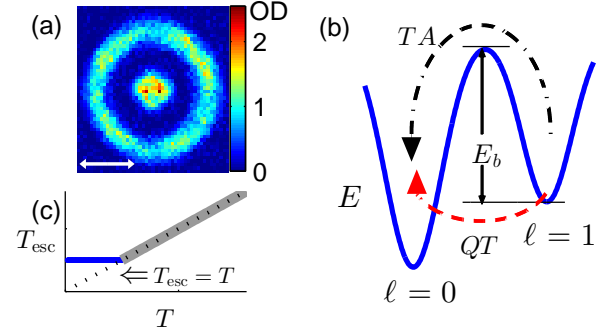


FIG. 1. Target shaped condensate, energy landscape and effective escape temperature (color online). a) *In situ* image of trapped atoms, with 5% of the total atoms imaged [20]. Experiments are performed on the ring-shaped BEC and the resulting winding number  $\ell$  is read out by interfering the ring condensate with the disc-shaped BEC in time of flight. The disc-shaped BEC acts as a phase reference. (b) Energy landscape showing the stationary state,  $\ell = 0$ , and the persistent current state,  $\ell = 1$ , as minima in the potential. The energy barrier  $E_b$  needs to be overcome for a persistent current to decay from  $\ell = 1$  to  $\ell = 0$ . The decay can be induced either via thermal activation (TA), or quantum tunneling (QT). (c) Crossover from quantum tunneling to the thermally activated regime. The escape temperature  $T_{\text{esc}}$  (see text) first remains constant (horizontal blue line) and then becomes equal to the physical temperature  $T$  (slanted gray line). A dotted line acts as a guide to the eye depicting  $T_{\text{esc}} = T$ .

ability and thus the escape temperature in quantum tunneling is independent of temperature, while for thermal activation, the escape temperature tracks the real temperature (Fig 1(c)). For our superfluid ring, the energy barrier  $E_b$  is much greater than all other energy scales in the problem, hence the lifetime of the persistent current is much greater than the experimental time-scale. However, the height of the energy barrier and the relative depth of the two wells can be changed by the addition of a density perturbation [11]. The density perturbation may induce a persistent current decay even if its strength is less than the chemical potential [6, 11].

In this paper, we measure the decay constant of a per-

\* gcampbe1@umd.edu

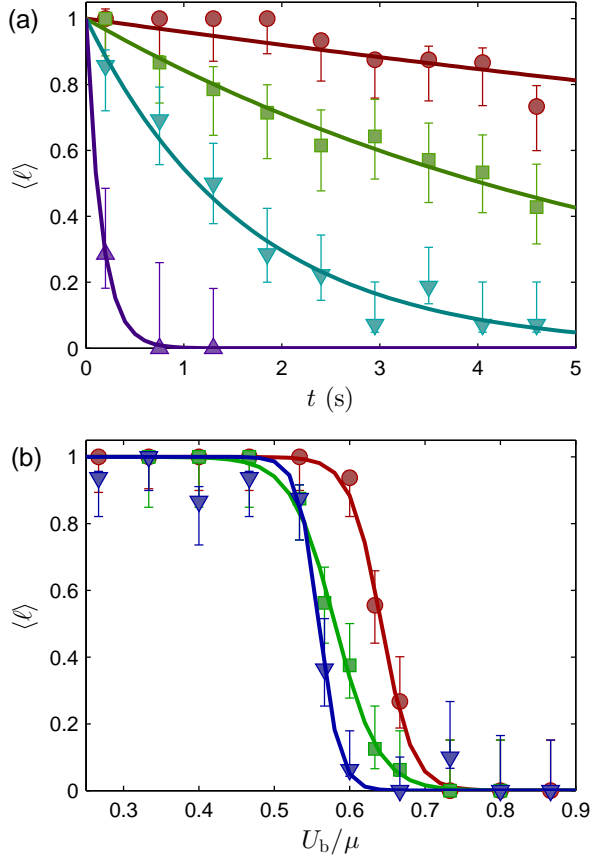


FIG. 2. (color online). (a) Average measured winding number  $\langle \ell \rangle$  vs.  $t$ , the duration for which a stationary perturbation is applied. The four data sets correspond to different strengths of the stationary perturbation  $U_b$ :  $0.50(5)\mu$  (circles),  $0.53(5)\mu$  (squares),  $0.56(6)\mu$  (inverted triangles) and  $0.59(6)\mu$  (triangles). Here,  $\mu$  is the unperturbed chemical potential. The temperature of the superfluid was  $85(20)$  nK. The solid curves show exponential fits. (b) The average measured winding number  $\langle \ell \rangle$  vs.  $U_b$  for fixed  $t$ :  $0.5$  s (circles),  $2.5$  s (squares) and  $4.5$  s (inverted triangles). The solid curves show a sigmoidal fit of the form  $\langle \ell \rangle = [\exp((U_b/\mu - \zeta)/\alpha) + 1]^{-1}$ . The temperature of the superfluid was  $40(12)$  nK.

sistent current for various perturbation strengths and temperatures. We also measure the size of hysteresis loops which allows us to extract the critical velocity, showing a clear effect of temperature on the critical velocity in a superfluid.

The preferred theoretical tool for modeling atomic condensates is the Gross-Pitaevskii (GP) equation, which is a zero-temperature, mean-field theory. Recent experiments exploring the effect of rotating perturbations on the critical velocity of toroidal superfluids have found both agreement [21, 22] and significant discrepancies [6, 11] between experimental results and GP calculations. Several non-zero temperature extensions to GP theory have been developed, including ZNG [23] and c-field [24]

[of which the Truncated Wigner approximation (TWA) is a special type]. To explore the role of temperature in phase slips in superfluid rings, Ref. [25] studied condensates confined to a periodic channel using TWA simulations. In addition, recent theoretical [26–32] and experimental [33] works explored a similar problem of dissipative vortex dynamics in a simply-connected trap.

Our experiment consists of a  $^{23}\text{Na}$  Bose-Einstein condensate (BEC) in a target-shaped optical dipole trap [34] [Fig. 1(a)]. The inner disc BEC has a measured Thomas-Fermi (TF) radius of  $7.9(1) \mu\text{m}$ . The outer toroid has a Thomas-Fermi full-width of  $5.4(1) \mu\text{m}$  and a mean radius of  $22.4(6) \mu\text{m}$ . To create the target potential, we image the pattern programmed on a digital micromirror device (DMD) onto the atoms while illuminating it with blue-detuned light. This allows us to create arbitrary potentials for the atoms. Vertical confinement is created either using a red-detuned  $\text{TEM}_{00}$  or a blue-detuned  $\text{TEM}_{01}$  beam. The potential generated by the combination of the red-detuned  $\text{TEM}_{00}$  beam and ring beam is deeper than that of blue-detuned  $\text{TEM}_{01}$  and ring beam; thus the temperature is generally higher in the red-detuned sheet potential. We use this feature to realize four different trapping configurations with temperatures  $T$  of  $30(10)$  nK,  $40(12)$  nK,  $85(20)$  nK and  $195(30)$  nK but all with roughly the same chemical potential of  $\mu/\hbar = 2\pi \times (2.7(2) \text{ kHz})$ . (See supplemental material for details about temperature and trapping configurations.) Finally, a density perturbation is created by another blue-detuned Gaussian beam with a  $1/e^2$  width of  $6 \mu\text{m}$  and can be rotated or held stationary at an arbitrary angle in the plane of the trap [35].

To probe the lifetime of the persistent current, we first initialize the ring-shaped BEC into the  $\ell = 1$  state with a fidelity of  $0.96(2)$  (see Supplemental material). A stationary perturbation with a strength  $U_b < \mu$  is then applied for a variable time  $t$  ranging from  $0.2$  s to  $4.6$  s. To compensate for the  $25(2)$  s lifetime of the condensate, we insert a variable length delay between the initialization step and application of the perturbation to keep the total time constant (Without this normalization, a  $25(2)$  s lifetime would cause an atom loss of  $\approx 20\%$  in  $4.7$  s, changing the chemical potential by  $\approx 10\%$ ). At the end of the experiment, the circulation state is measured by releasing the atoms and looking at the resulting interference pattern between the ring and disc BECs [11, 36]. For each temperature, four different perturbation strengths are selected. The perturbation strengths are chosen such that the lifetime of the persistent current state is varied over the entire range of  $t$ . The measurement is repeated 16–18 times for each combination of  $U_b$ ,  $T$  and  $t$ . The average of the measured circulation states  $\langle \ell \rangle$  gives the probability of the circulation state surviving for a given set of experimental parameters.

Figure 2(a) shows  $\langle \ell \rangle$  vs.  $t$  for  $T = 85(20)$  nK and four different  $U_b$ . We fit the data to an exponential  $\exp(-\Gamma t)$ . GP theory predicts either a fast decay ( $< 10$  ms) or no decay, depending on the precise value of  $U_b/\mu$  [25]. By

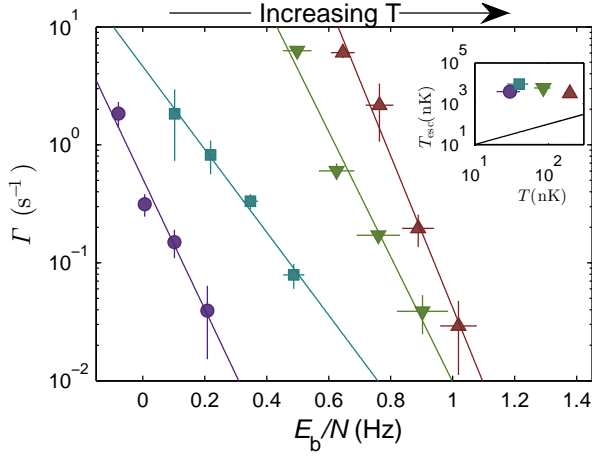


FIG. 3. (color online). Measured decay rate of the persistent current  $\Gamma$  as a function of perturbation strength  $U_b$  for four different temperatures: 30(10) nK (circles), 40(12) nK (squares), 85(20) nK (inverted circles) and 195(30) nK (triangles). The solid lines are fits of the form  $\Gamma = \Omega_a \exp(E_b/k_B T_{\text{esc}})$ , where  $E_b$  is the energy barrier,  $k_B$  is the Boltzmann constant, and  $T_{\text{esc}}$  and  $\Omega_a$  are fit parameters. The inset shows the extracted  $T_{\text{esc}}$  as a function of measured physical temperature: 30(10) nK (triangle), 40(12) nK (square), 85(20) nK (circle) and 195(30) nK (inverted triangle). The solid line shows  $T_{\text{esc}} = T$ .

contrast, we see from Fig. 2(a) that  $\Gamma$  changes smoothly from  $4.1(6) \times 10^{-2} \text{ s}^{-1}$  to  $6.2(8) \text{ s}^{-1}$  as  $U_b$  is changed from  $0.50(4)\mu$  to  $0.59(5)\mu$ . Thus we are able to tune the decay rate by over two orders of magnitude by changing the magnitude of perturbation by  $\approx 0.1\mu$ , in qualitative agreement with TWA simulation results [25]. This confirms that the decay of a persistent current is a probabilistic process, in contrast to the instantaneous, deterministic transitions seen in GPE simulations [25].

To explore whether a longer hold time shifts or broadens the transition between persistent current states, we measured the average persistent current as a function of  $U_b$  while keeping  $t$  constant. Figure 2(b) shows this measurement for three different  $t$ : 0.5 s, 2.5 s and 4.5 s. We fit this data to a sigmoidal function of the form  $\langle \ell \rangle = [\exp((U_b/\mu - \zeta)/\alpha) + 1]^{-1}$  to extract estimates of the width  $\alpha$  and center  $\zeta$  of the transition [37]. We see that changing the perturbation strength by  $\approx 0.2\mu$  decreases  $\langle \ell \rangle$  from one to zero. The width  $\alpha$  is essentially unchanged as we change  $t$  from 0.5 s to 4.5 s, though the center of the sigmoid  $\zeta$  shifts by  $\approx 0.1U_b/\mu$ . We also took similar measurements at a temperature of 85(20) nK (not shown). The width  $\alpha$  remains essentially independent of  $t$  even at higher temperatures. For a hold time  $t = 0.5$  s, we found a center  $\zeta = 0.50(4)U_b/\mu$  at  $T = 85(20)$  nK; by contrast, we obtain  $\zeta = 0.64(4)U_b/\mu$  for a  $T = 40(12)$  nK. This indicates that an increase in temperature makes a phase slip more probable even with smaller  $U_b$ .

To understand if the decay of the persistent current is thermally activated or quantum mechanical in nature, we

first must understand the nature of the energy barrier,  $E_b$ , that separates the two states. To estimate the size of  $E_b$ , we consider excitations that connect the  $\ell = 1$  to the  $\ell = 0$  state. In the context of a one-dimensional ring, a persistent current decay corresponds to having fluctuations reduce the local density, producing a soliton that subsequently causes a phase slip [38]. For rings with non-negligible radial extent, TWA simulations suggest that a vortex passing through the annulus of the ring (through the perturbation region) causes the transition [25]. Because of the narrow width of our ring, we expect that a solitonic-vortex is the lowest energy excitation that can connect two persistent current states [39–44]. An analytical form for the energy of a solitonic vortex is given by [40, 41]:

$$\epsilon_{sv}(U_b/\mu) \approx \pi n_{2D} \frac{\hbar^2}{m} \ln\left(\frac{R_\perp}{\xi}\right) + \frac{1}{2} m N_c \left(\frac{\hbar}{2mR}\right)^2 \quad (1)$$

where  $N_c$  is the total number of condensate atoms in the ring,  $\xi$  is the healing length,  $R_\perp$  is the Thomas-Fermi width of the perturbation region and  $n_{2D}$  is the maximum 2D density in the region of the perturbation. The first term is the energy of a solitonic-vortex while the second term is the kinetic energy of the remaining  $\pi$  phase winding around the ring. We note that  $N_c$ ,  $R_\perp$ ,  $\xi$  and  $n_{2D}$  all depend implicitly on  $T$  and  $U_b$ . Finally,

$$E_b(U_b, T) = \epsilon_{sv} - \epsilon_{\ell=1} = \epsilon_{sv} - \frac{1}{2} m N_c \left(\frac{\hbar}{mR}\right)^2, \quad (2)$$

where  $\epsilon_{\ell=1}$  is the energy of the first persistent current state. We have verified the accuracy of these expressions using GP calculations similar to those in Refs. [40, 41, 45, 46] to within 10 % for our parameters.

Fig. 3 shows the clear temperature dependence of the measured decay rate  $\Gamma$  of the persistent current. To quantify this dependence, we fit the data to the form  $\Gamma = \Omega_a \exp(-E_b/k_B T_{\text{esc}})$  for each temperature (shown as the solid lines in Fig. 3). We note that while the attempt frequency  $\Omega_a$  is dependent on temperature (changing by five orders of magnitude from 40(12) nK to 195(30) nK),  $T_{\text{esc}}$  is not (see inset of Fig. 3). In fact,  $T_{\text{esc}}$  is roughly constant at  $\approx 3\mu\text{K}$ , while the BEC temperature varies from 30(10) nK to 195(30) nK. The constancy of  $T_{\text{esc}}$  with real  $T$  hints that a temperature-independent phenomenon sets the probability for tunneling on any given attempt. A similar effect was seen in superconductors [19], and is understood to be macroscopic quantum tunneling. We can estimate the decay rate due to quantum tunneling by drawing an analogy with an rf-superconducting quantum interference device. In this device, the quantum tunneling rate can be estimated by the WKB approximation,  $\Gamma_q \approx (\omega_p/2\pi) \exp(-E_b/\hbar\omega_p)$ , where  $\omega_p$  is the frequency of the first photon mode in the superconducting system [14]. Here, by analogy,  $\omega_p$  is the frequency of the first azimuthal phonon mode, which is  $\approx 2\pi \times 30$  Hz. For our system,  $E_b/\hbar\omega_p > 10^3$ , so  $\Gamma_q \approx (\omega_p/2\pi) \exp(-10^3)$ , implying that quantum tunneling should be negligible.

FIG. 4. Hysteresis loop for a perturbation strength of  $0.64(4)U_b/\mu$  for 40(12) nK (a), 85(20) nK (b), and 195(30) nK (c). (d) Size of the hysteresis loop,  $(\Omega_+ - \Omega_-)/\Omega_0$  (see text), vs. barrier strength for three different temperatures: 40(12) nK, diamonds, 85(12) nK (squares), and 195(12) nK (triangles). The zero temperature, GPE predicted, area of the hysteresis loop is shown as a purple band, which incorporates the uncertainty in speed of sound. The left y axis of the inset shows the hysteresis loop size shown in (a)-(c) as a function of temperature for a perturbation strength of  $0.64(4)U_b/\mu$ . The numbers to the right right show the corresponding extracted critical velocity  $v_c$  in (mm/s).

Thus, the observed decay cannot be described by either simple thermal activation or quantum mechanical tunneling. It may be that more complicated models of energy dissipation may be required.

Finally, because there are parallels between a vortex moving through the annulus of the ring and a vortex leaving a simply connected BEC, we investigated models that predict the dissipative dynamics of these vortices [30, 32]. Such models predict lifetimes that scale algebraically with  $E_b$  and  $T$ . As can be seen from Fig. 3 our data scales exponentially with  $E_b$ . Thus, these models fail to explain the experimental data.

The measurements of the decay constants described above shows the strong effect of temperature on the persistent current state. As discussed above, this temperature dependence is wholly captured in the variation of the constant  $\Omega_a$  with  $T$ , as  $T_{\text{esc}}$  is constant. This causes an apparent change in the critical velocity of a moving

barrier (for a given application time), with higher temperatures having lower critical velocities. Such a change in critical velocity affects hysteresis loops [11]. For initial circulation state  $\ell = 0(1)$ , we experimentally determine  $\Omega_+(\Omega_-)$ , the angular velocity of the perturbation at which  $\langle \ell \rangle = 0.5$ . The hysteresis loop size is given by  $\Omega_+ - \Omega_-$ , normalized to  $\Omega_0$ , where  $\Omega_0 = \hbar/mR^2$ ,  $m$  is the mass of an atom,  $R$  is the mean radius of the torus. We measure the hysteresis loop for four perturbation strengths and three different temperatures: 40(10) nK, 85(20) nK and 195(30) nK as shown in Fig. 4, with the zero-temperature GP prediction based on the speed of sound shown for references [11, 47]. We see from Fig. 4 that the discrepancy between experimental data and theoretical predictions decreases as the temperature is lowered. Using the density distribution of atoms around the ring, we extract the critical velocity from the hysteresis loop size [11]. For example, at  $U_b/\mu = 0.64(4)$ , a temperature change of 40(12) nK to 195(30) nK corresponds to a change in the critical velocity of  $0.26(6) c_s$  to  $0.03(2) c_s$ . Here,  $c_s$  is the speed of sound in the bulk. While the measured critical velocity approached the zero-temperature, speed of sound, we see that at non-zero temperature thermal fluctuations must be taken into account in any measurement or calculation of the critical velocity.

In conclusion, we have measured the effect of temperature on transitions between persistent current states in a ring condensate in the presence of a local perturbation. The results of this work indicate that as thermal fluctuations become more pronounced, it becomes easier for the superfluid to overcome the energy barrier and the persistent current state to decay. If we assume that the decay is thermally driven and is thus described by an Arrhenius-type equation, we find a significant discrepancy between the measured temperature and the effective temperature governing the decay. Other possible mechanisms like macroscopic quantum tunneling should be greatly suppressed. Despite the disagreement, we find a clear temperature dependence of the critical velocity of the superfluid by measuring hysteresis loops. This work will provide a benchmark for finite temperature calculations on the decay of topological excitation in toroidal superfluids.

## ACKNOWLEDGMENTS

The authors thank M. Edwards, M. Davis, A. Yaki-menko, and W.D. Phillips for useful discussions. This work was partially supported by ONR, the ARO atom-tronics MURI, and the NSF through the PFC at the JQI.

[1] H. K. Onnes, Koninkl. Ned. Akad. Wetenschap. **23**, 278 (1914).  
[2] J. File and R. G. Mills, *Phys. Rev. Lett.* **10**, 93 (1963).

[3] J. B. Mehl and W. Zimmermann, *Phys. Rev.* **167**, 214 (1968).  
[4] I. Rudnick, H. Kojima, W. Veith, and R. S. Kagiwada,

- Phys. Rev. Lett. **23**, 1220 (1969).
- [5] C. Ryu, M. F. Andersen, P. Cladé, V. Natarajan, K. Helmerson, and W. D. Phillips, *Phys. Rev. Lett.* **99**, 260401 (2007).
- [6] A. Ramanathan, K. C. Wright, S. R. Muniz, M. Zelan, W. T. Hill, C. J. Lobb, K. Helmerson, W. D. Phillips, and G. K. Campbell, *Phys. Rev. Lett.* **106**, 130401 (2011).
- [7] S. Beattie, S. Moulder, R. J. Fletcher, and Z. Hadzibabic, *Phys. Rev. Lett.* **110**, 025301 (2013).
- [8] D. Sanvito, F. M. Marchetti, M. H. Szymańska, G. Tosi, M. Baudisch, F. P. Laussy, D. N. Krizhanovskii, M. S. Skolnick, L. Marrucci, A. Lemaître, J. Bloch, C. Tejedor, and L. Viña, *Nature Physics* **6**, 527 (2010).
- [9] R. Doll and M. Näbauer, *Phys. Rev. Lett.* **7**, 51 (1961).
- [10] E. J. Mueller, *Phys. Rev. A* **66**, 063603 (2002).
- [11] S. Eckel, J. G. Lee, F. Jendrzejewski, N. Murray, C. W. Clark, C. J. Lobb, W. D. Phillips, M. Edwards, and G. K. Campbell, *Nature (London)* **506**, 200 (2014).
- [12] A. Caldeira and A. Leggett, *Annals of Physics* **149**, 374 (1983).
- [13] J. M. Martinis, M. H. Devoret, and J. Clarke, *Phys. Rev. Lett.* **55**, 1543 (1985).
- [14] J. Clarke, A. N. Cleland, M. H. Devoret, D. Esteve, and J. Martinis, *Science* **239**, 992 (1988).
- [15] J. M. Martinis and H. Grabert, *Phys. Rev. B* **38**, 2371 (1988).
- [16] R. Rouse, S. Han, and J. E. Lukens, *Phys. Rev. Lett.* **75**, 1614 (1995).
- [17] D. B. Schwartz, B. Sen, C. N. Archie, and J. E. Lukens, *Phys. Rev. Lett.* **55**, 1547 (1985).
- [18] F. Sharifi, J. L. Gavilano, and D. J. Van Harlingen, *Phys. Rev. Lett.* **61**, 742 (1988).
- [19] R. F. Voss and R. A. Webb, *Phys. Rev. Lett.* **47**, 265 (1981).
- [20] A. Ramanathan, S. R. Muniz, K. C. Wright, R. P. Anderson, W. D. Phillips, K. Helmerson, and G. K. Campbell, *Review of Scientific Instruments* **83**, 083119 (2012).
- [21] F. Jendrzejewski, S. Eckel, N. Murray, C. Lanier, M. Edwards, C. J. Lobb, and G. K. Campbell, *Phys. Rev. Lett.* **113**, 045305 (2014).
- [22] C. Ryu, P. W. Blackburn, A. A. Blinova, and M. G. Boshier, *Phys. Rev. Lett.* **111**, 205301 (2013).
- [23] E. Zaremba, T. Nikuni, and A. Griffin, *Journal of Low Temperature Physics* **116**, 277 (1999).
- [24] P. Blakie, A. Bradley, M. Davis, R. Ballagh, and C. Gardiner, *Advances in Physics* **57**, 363 (2008).
- [25] A. C. Mathey, C. W. Clark, and L. Mathey, *Phys. Rev. A* **90**, 023604 (2014).
- [26] S. J. Rooney, A. S. Bradley, and P. B. Blakie, *Phys. Rev. A* **81**, 023630 (2010).
- [27] S. J. Rooney, A. J. Allen, U. Zülicke, N. P. Proukakis, and A. S. Bradley, *Phys. Rev. A* **93**, 063603 (2016).
- [28] M. Kobayashi and M. Tsubota, *Phys. Rev. Lett.* **97**, 145301 (2006).
- [29] B. Jackson, N. Proukakis, C. Barenghi, and E. Zaremba, *Phys. Rev. A* **79**, 053615 (2009).
- [30] R. A. Duine, B. W. A. Leurs, and H. T. C. Stoof, *Phys. Rev. A* **69**, 053623 (2004).
- [31] N. Berloff and A. Youd, *Phys. Rev. Lett.* **99**, 145301 (2007).
- [32] P. O. Fedichev and G. V. Shlyapnikov, *Phys. Rev. A* **60**, R1779 (1999).
- [33] G. Moon, W. J. Kwon, H. Lee, and Y.-i. Shin, *Phys. Rev. A* **92**, 051601 (2015).
- [34] S. Eckel, F. Jendrzejewski, A. Kumar, C. J. Lobb, and G. K. Campbell, *Phys. Rev. X* **4**, 031052 (2014).
- [35] K. C. Wright, R. B. Blakestad, C. J. Lobb, W. D. Phillips, and G. K. Campbell, *Phys. Rev. Lett.* **110**, 025302 (2013).
- [36] L. Corman, L. Chomaz, T. Bienaimé, R. Desbuquois, C. Weitenberg, S. Nascimbène, J. Dalibard, and J. Beugnon, *Phys. Rev. Lett.* **113**, 135302 (2014).
- [37] The extracted center and FWHM of the transition are independent of the form of the sigmoidal function chosen.
- [38] W. A. Little, *Phys. Rev.* **156**, 396 (1967).
- [39] J. Brand and W. P. Reinhardt, *Journal of Physics B: Atomic, Molecular and Optical Physics* **34**, L113 (2001).
- [40] A. M. Mateo and J. Brand, *New Journal of Physics* **17**, 125013 (2015).
- [41] M. J. H. Ku, W. Ji, B. Mukherjee, E. Guardado-Sanchez, L. W. Cheuk, T. Yefsah, and M. W. Zwierlein, *Phys. Rev. Lett.* **113**, 065301 (2014).
- [42] G. Valtolina, A. Burchianti, A. Amico, E. Neri, K. Xhani, J. A. Seman, A. Trombettoni, A. Smerzi, M. Zaccanti, M. Inguscio, and G. Roati, *Science* **350**, 1505 (2015).
- [43] S. Donadello, S. Serafini, M. Tylutki, L. P. Pitaevskii, F. Dalfovo, G. Lamporesi, and G. Ferrari, *Phys. Rev. Lett.* **113**, 065302 (2014).
- [44] M. Tylutki, S. Donadello, S. Serafini, L. P. Pitaevskii, F. Dalfovo, G. Lamporesi, and G. Ferrari, *The European Physical Journal Special Topics* **224**, 577 (2015).
- [45] J. Brand and W. P. Reinhardt, *Phys. Rev. A* **65**, 043612 (2002).
- [46] S. Komineas and N. Papanicolaou, *Phys. Rev. A* **68**, 043617 (2003).
- [47] G. Watanabe, F. Dalfovo, F. Piazza, L. P. Pitaevskii, and S. Stringari, *Phys. Rev. A* **80**, 053602 (2009).